

Homotopy Relaxation Training Algorithms for Infinite-Width Two-Layer ReLU Neural Networks

Yahong Yang · Qipin Chen · Wenrui Hao

Received: date / Accepted: date

Abstract In this paper, we present a novel training approach called the Homotopy Relaxation Training Algorithm (HRTA), aimed at accelerating the training process in contrast to traditional methods. Our algorithm incorporates two key mechanisms: one involves building a homotopy activation function that seamlessly connects the linear activation function with the ReLU activation function; the other technique entails relaxing the homotopy parameter to enhance the training refinement process. We have conducted an in-depth analysis of this novel method within the context of the neural tangent kernel (NTK), revealing significantly improved convergence rates. Our experimental results, especially when considering networks with larger widths, validate the theoretical conclusions. This proposed HRTA exhibits the potential for other activation functions and deep neural networks.

Keywords Neural Networks · Homotopy · Relaxation · Optimization

Mathematics Subject Classification (2020) 68T07 · 68W10 · 65K99

YY and WH are supported by National Institute of General Medical Sciences through grant 1R35GM146894.

Yahong Yang
Department of Mathematics, The Pennsylvania State University, University Park, State College, PA 16802, USA
E-mail: yxy5498@psu.edu

Qipin Chen
Amazon Prime Video, Seattle, MA 98109, USA
E-mail: qipinche@amazon.com

Wenrui Hao
Department of Mathematics, The Pennsylvania State University, University Park, State College, PA 16802, USA
E-mail: wxh64@psu.edu

1 Introduction

Neural networks (NNs) with the rectified linear unit (ReLU) activation function [12, 3] have become increasingly popular in scientific and engineering applications, such as image classification [26, 16], regularization [17, 43]. Finding an efficient way to train and obtain the parameters in NNs is an important task, enabling the application of NNs in various domains.

Numerous studies have delved into training methods for NNs, as evidenced by the works of [10, 24, 46, 15, 27, 29, 25, 41, 42, 34, 35, 38]. However, the optimization of loss functions can become increasingly challenging over time, primarily due to the nonconvex energy landscape. Traditional algorithms such as the gradient descent method and the Adam method often lead to parameter entrapment in local minima or saddle points for prolonged periods. The homotopy training algorithm (HTA) was introduced as a remedy by making slight modifications to the NN structure. HTA draws its roots from the concept of homotopy continuation methods [32, 36, 13, 14], with its initial introduction found in [6]. However, constructing a homotopy function requires it to be aligned with the structure of neural networks and entails time-consuming training.

In this paper, we introduce an innovative training approach called the homotopy relaxation training algorithm (HRTA). This approach leverages the homotopy concept, specifically focusing on the activation function, to address the challenges posed by the HRTA. We develop a homotopy activation function that establishes a connection between the linear activation function and the target activation function. By gradually adjusting the homotopy parameter, we enable a seamless transition toward the target activation function. Mathematically, the homotopy activation function is defined as σ_s , where s is the homotopy parameter, and it takes the form $\sigma_s(x) = (1-s)\text{Id}(x) + s\sigma(x)$. Here, $\text{Id}(x)$ represents the identity function (i.e., the linear activation function), and $\sigma(x)$ is the target activation function. The term ‘‘homotopy’’ in the algorithm signifies its evolution from an entirely linear neural network, where the initial activation function is the identity function ($s = 0$). The homotopy activation function undergoes gradual adjustments until it transforms into a target neural network ($s = 1$). This transition, from the identity function to the target function, mirrors the principles of homotopy methods. Furthermore, our analysis reveals that by extrapolating (or over-relaxing) the homotopy parameter ($1 < s < 2$), training performance can be further enhanced. In this context, we extend the concept of homotopy training, introducing what we refer to as ‘‘homotopy relaxation training.’’

In this paper, we relax the homotopy parameter and allow s to take on any positive value in $[0, 2]$, rather than being restricted to values in $[0, 1]$. Moreover, we provide theoretical support for this algorithm, particularly in hyperparameter scenarios. Our analysis is closely related to neural tangent kernel methods [20, 4, 48, 5, 9, 19, 7, 45, 33, 11, 2]. In contrast to classical neural tangent kernel methods, our algorithm studies training performance with changing activation functions during training. In other words, while classical neural tangent kernel methods focus on single neural networks, our algorithm allows for

changes in the structure of the neural network due to changes in the activation function during the training. There are other works that introduce parameters during training. They learn the activation during training and identify an adaptive activation function, as demonstrated in [21, 22, 23, 1]. However, these methods differ from ours. In their approach, they find the proper activation during training, implying a single iteration. The loss function can only decay in one iteration, without another chance to decay. The concept of homotopy in our paper lies in not needing to learn the active function explicitly; instead, we propose a method to alter the function. The loss function has multiple opportunities to decay as we modify the energy landscape between different iterations. We establish that modifying the homotopy parameter at each step increases the smallest eigenvalue of the gradient descent kernel for infinite-width neural networks (see Theorem 1). Consequently, we present Theorem 2 to demonstrate the capacity of HRTA to enhance training speed.

The paper is organized as follows: We introduce the HRTA in Section 2. Next, in Section 3, we provide theoretical support for our theory. Finally, in Section 4, we conduct experiments, including supervised learning and solving partial differential equations, based on our algorithm.

2 Homotopy Relaxation Training Algorithm

In this paper, we consider supervised learning for NNs. Within a conventional supervised learning framework, the primary objective revolves around acquiring an understanding of a high dimensional target function denoted as $f(\mathbf{x})$ in $[0, 1]^d$, with $\|f\|_{L_\infty([0, 1]^d)} \leq 1$, through a finite collection of data samples $\{(\mathbf{x}_i, f(\mathbf{x}_i))\}_{i=1}^n$. When embarking on the training of a NN, our aim rests upon the discovery of a NN representation denoted as $\phi(\mathbf{x}; \boldsymbol{\theta})$ that serves as an approximation to $f(\mathbf{x})$, a feat achieved through the utilization of randomly gathered data samples $\{(\mathbf{x}_i, f(\mathbf{x}_i))\}_{i=1}^n$, with $\boldsymbol{\theta}$ representing the parameters within the NN architecture. It is assumed, in this paper, that the sequence $\{\mathbf{x}_i\}_{i=1}^n$ constitutes an independent and identically distributed (i.i.d.) sequence of random variables, uniformly distributed across $[0, 1]^d$. Denote

$$\boldsymbol{\theta}_S := \arg \min_{\boldsymbol{\theta}} \mathcal{R}_S(\boldsymbol{\theta}) := \arg \min_{\boldsymbol{\theta}} \frac{1}{2n} \sum_{i=1}^n |f(\mathbf{x}_i) - \phi(\mathbf{x}_i; \boldsymbol{\theta})|^2. \quad (1)$$

Next, we introduce the HRTA by defining $\sigma_{s_p}(x) = (1 - s_p)\text{Id}(x) + s_p\sigma(x)$ with a discretized set points of the homotopy parameter $\{s_p\}_{p=1}^M \subset (0, 2)$. We then proceed to obtain:

$$\boldsymbol{\theta}_S^{s_p} := \arg \min_{\boldsymbol{\theta}} \mathcal{R}_{S, s_p}(\boldsymbol{\theta}), \text{ with an initial guess } \boldsymbol{\theta}_S^{s_{p-1}}, p = 1, \dots, M, \quad (2)$$

where we initialize $\boldsymbol{\theta}_S^{s_0}$ randomly, and $\boldsymbol{\theta}_S^{s_M}$ represents the optimal parameter value that we ultimately achieve.

In this paper, we consider a two-layer NN defined as follows

$$\phi(\mathbf{x}; \boldsymbol{\theta}) := \frac{1}{\sqrt{m}} \sum_{k=1}^m a_k \sigma(\boldsymbol{\omega}_k^T \mathbf{x}), \quad (3)$$

with the activation function $\sigma(z) = \text{ReLU}(z) = \max\{z, 0\}$. The evolution of the traditional training can be written as the following differential equation:

$$\frac{d\boldsymbol{\theta}(t)}{dt} = -\nabla_{\boldsymbol{\theta}} \mathcal{R}_S(\boldsymbol{\theta}(t)). \quad (4)$$

In the HRTA setup, we train a sequences of leaky ReLU activate functions [44, 31]. Subsequently, for each of these Leaky ReLUs with given s_p , we train the neural network on a time interval of $[t_{p-1}, t_p]$:

$$\frac{d\boldsymbol{\theta}(t)}{dt} = -\nabla_{\boldsymbol{\theta}} \mathcal{R}_{S, s_p}(\boldsymbol{\theta}(t)). \quad (5)$$

Moreover, we have $t_0 = 0$ and initialize the parameter vector $\boldsymbol{\theta}(0)$, drawn from a normal distribution $\mathcal{N}(\mathbf{0}, \mathbf{I})$. Therefore the HRTA algorithm's progression is outlined in **Algorithm 1**.

Remark 1 If $s_M = 1$, then upon completion, we will have obtained $\boldsymbol{\theta}(t_M)$ and the NN $\phi_{s_M}(\mathbf{x}; \boldsymbol{\theta}(t_M))$, characterized by pure ReLU activations. The crux of this algorithm is its ability to transition from Leaky ReLUs to a final configuration of a NN with pure ReLU activations. This transformation is orchestrated via a series of training iterations utilizing the homotopy approach.

However, our paper demonstrates that there is no strict necessity to achieve $s_M = 1$. What we aim for is to obtain a NN with parameters $\boldsymbol{\theta}$ that minimizes $\mathcal{R}_{S, s_M}(\boldsymbol{\theta})$. This is because, for any value of s , we can readily represent $\phi_s(\mathbf{x}; \boldsymbol{\theta})$ as a pure ReLU NN, as shown in the following equation:

$$\begin{aligned} \sigma_s(x) &= (1-s)\text{Id}(x) + s\sigma(x) \\ &= (1-s)\sigma(x) - (1-s)\sigma(-x) + s\sigma(x) = \sigma(x) - (1-s)\sigma(-x). \end{aligned}$$

To put it simply, if we can effectively train a NN with Leaky-ReLU to learn the target functions, it implies that we can achieve the same level of performance with a NN using standard ReLU activation. Consequently, the theoretical analysis in the paper does not require that the final value of s_M must be set to 1. Moreover, our method is applicable even when $s_M > 1$, which we refer to as the relaxation part of HRTA. It's important to highlight that for $s > 1$ the decay speed may surpass that of a pure ReLU neural network. This is consistent with the training using the hat activation function (specifically, when $s = 2$ in the homotopy activation function) discussed in [18]. , although it's worth noting that their work primarily focuses on the linear case (involving only the constant factor change), whereas our work extends this consideration to neural networks.

Algorithm 1: The Homotopy Training Algorithm for Two Layer Neural Networks

input : Sample points of function $\{(\mathbf{x}_i, f(\mathbf{x}_i))\}_{i=1}^n$; Initialized homotopy parameter $s_1 > 0$; Number of the iteration times M ; $\zeta > 0$; Training time of each iteration T ; $t_p = pT$; learning rate τ ; $\boldsymbol{\theta}_0 \sim \mathcal{N}(0, \mathbf{I})$.

- 1 **for** $p = 1, 2, \dots, M$ **do**
- 2 **for** $t \in [t_{p-1}, t_p]$ **do**
- 3 $\boldsymbol{\theta}_{t+\tau} = \boldsymbol{\theta}_t - \tau \nabla_{\boldsymbol{\theta}}(\mathcal{R}_{s_p}(\boldsymbol{\theta}_t))$;
- 4 **end**
- 5 $s_{p+1} := s_p + \zeta$;
- 6 **end**

output: $\phi_{s_M}(\mathbf{x}, \boldsymbol{\theta}_{T_M})$ as the two layer NN approximation to approximate $f(\mathbf{x})$.

3 Convergence Analysis

In this section, we will delve into the convergence analysis of the HRTA based on the neural target kernel methods [20, 4, 48, 5, 9, 19, 7, 45, 33, 11, 2]. For simplicity, we will initially focus on the case where $M = 2$. Note that for cases with $M > 2$, all analyses presented here can be readily extended by repeating the analysis from the first iteration to the second iteration. To start, we set the initial value of $s_1 > 0$. The structure of the proof of Theorem 2 is shown in Figure 1.

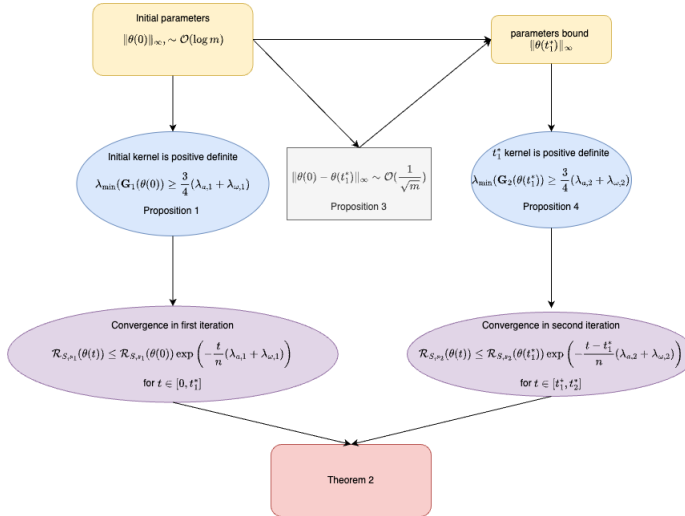


Fig. 1 Structure of proof of Theorem 2

3.1 Preliminaries

3.1.1 Neural networks

Let us summarize all basic notations used in the NNs as follows:

1. Matrices are denoted by bold uppercase letters. For example, $\mathbf{A} \in \mathbb{R}^{m \times n}$ is a real matrix of size $m \times n$ and \mathbf{A}^T denotes the transpose of \mathbf{A} . $\|\mathbf{A}\|_F$ is the Frobenius norm of the matrix \mathbf{A} .

2. Vectors are denoted by bold lowercase letters. For example, $\mathbf{v} \in \mathbb{R}^n$ is a column vector of size n .

3. Assume $\mathbf{n} \in \mathbb{N}_+^n$, then $f(\mathbf{n}) = \mathcal{O}(g(\mathbf{n}))$ means that there exists positive C independent of \mathbf{n}, f, g such that $f(\mathbf{n}) \leq Cg(\mathbf{n})$ when all entries of \mathbf{n} go to $+\infty$.

4. Recall $\sigma(x) = \max\{0, x\}$ and $\sigma_s(x) = (1-s)\text{Id}(x) + s\sigma(x)$ for $s > 0$. Two-layer NN structures are defined by:

$$\phi_{s_p}(\mathbf{x}; \boldsymbol{\theta}) := \frac{1}{\sqrt{m}} \sum_{k=1}^m a_k \sigma_{s_p}(\boldsymbol{\omega}_k^T \mathbf{x}). \quad (6)$$

5. Recall that

$$\mathcal{R}_{S, s_p}(\boldsymbol{\theta}) := \frac{1}{2n} \sum_{i=1}^n |f(\mathbf{x}_i) - \phi_{s_p}(\mathbf{x}_i; \boldsymbol{\theta})|^2, \quad (7)$$

it is assumed that the sequence $\{\mathbf{x}_i\}_{i=1}^n$ consists of independent and identically distributed (i.i.d.) random variables. These random variables are uniformly distributed within the hypercube $[0, 1]^d$, where d is the dimension of the input space.

3.2 Gradient descent kernel

The kernels characterizing the training dynamics for the p -th iteration take the following form:

$$\begin{aligned} k_p^{[a]}(\mathbf{x}, \mathbf{x}') &:= \mathbf{E}_{\boldsymbol{\omega}} \sigma_{s_p}(\boldsymbol{\omega}^T \mathbf{x}) \sigma_{s_p}(\boldsymbol{\omega}^T \mathbf{x}') \\ k_p^{[\omega]}(\mathbf{x}, \mathbf{x}') &:= \mathbf{E}_{(a, \boldsymbol{\omega})} a^2 \sigma'_{s_p}(\boldsymbol{\omega}^T \mathbf{x}) \sigma'_{s_p}(\boldsymbol{\omega}^T \mathbf{x}') \mathbf{x} \cdot \mathbf{x}'. \end{aligned} \quad (8)$$

The Gram matrices, denoted as $\mathbf{K}_p^{[a]}$ and $\mathbf{K}_p^{[\omega]}$, corresponding to an infinite-width two-layer network with the activation function σ_{s_p} , can be expressed as follows:

$$\begin{aligned} K_{ij,p}^{[a]} &= k_p^{[a]}(\mathbf{x}_i, \mathbf{x}_j), \quad \mathbf{K}_p^{[a]} = (K_{ij,p}^{[a]})_{n \times n}, \\ K_{ij,p}^{[\omega]} &= k_p^{[\omega]}(\mathbf{x}_i, \mathbf{x}_j), \quad \mathbf{K}_p^{[\omega]} = (K_{ij,p}^{[\omega]})_{n \times n} \end{aligned} \quad (9)$$

Moreover, the Gram matrices, referred to as $\mathbf{G}_p^{[a]}$ and $\mathbf{G}_p^{[\omega]}$, corresponding to a finite-width two-layer network with the activation function σ_{s_p} , can be defined as

$$\begin{aligned} G_{ij,p}^{[a]} &= \frac{1}{m} \sum_{k=1}^m \sigma_{s_p}(\boldsymbol{\omega}_k^T \mathbf{x}) \sigma_{s_p}(\boldsymbol{\omega}_k^T \mathbf{x}'), \quad \mathbf{G}_p^{[a]} = (G_{ij,p}^{[a]})_{n \times n}, \\ G_{ij,p}^{[\omega]} &= \frac{1}{m} \sum_{k=1}^m a^2 \sigma'_{s_p}(\boldsymbol{\omega}_k^T \mathbf{x}) \sigma'_{s_p}(\boldsymbol{\omega}_k^T \mathbf{x}') \mathbf{x} \cdot \mathbf{x}', \quad \mathbf{K}_p^{[\omega]} = (G_{ij,p}^{[\omega]})_{n \times n}. \end{aligned} \quad (10)$$

Assumption 1 Denote $\mathbf{K}^{[a]}$ and $\mathbf{K}^{[\omega]}$ are the Gram matrices for ReLU neural network and

$$\begin{aligned} H_{ij}^{[a]} &= k^{[a]}(-\mathbf{x}_i, \mathbf{x}_j), \quad \mathbf{H}^{[a]} = (H_{ij}^{[a]})_{n \times n}, \quad H_{ij}^{[\omega]} = k^{[\omega]}(-\mathbf{x}_i, \mathbf{x}_j), \quad \mathbf{H}^{[\omega]} = (H_{ij}^{[\omega]})_{n \times n} \\ M_{ij}^{[a]} &= k^{[a]}(\mathbf{x}_i, -\mathbf{x}_j), \quad \mathbf{M}^{[a]} = (M_{ij}^{[a]})_{n \times n}, \quad M_{ij}^{[\omega]} = k^{[\omega]}(\mathbf{x}_i, -\mathbf{x}_j), \quad \mathbf{M}^{[\omega]} = (M_{ij}^{[\omega]})_{n \times n} \\ T_{ij}^{[a]} &= k^{[a]}(-\mathbf{x}_i, -\mathbf{x}_j), \quad \mathbf{T}^{[a]} = (T_{ij}^{[a]})_{n \times n}, \quad T_{ij}^{[\omega]} = k^{[\omega]}(-\mathbf{x}_i, -\mathbf{x}_j), \quad \mathbf{T}^{[\omega]} = (T_{ij}^{[\omega]})_{n \times n}. \end{aligned}$$

Suppose that all matrices defined above are strictly positive definite.

Remark 2 We would like to point out that if, for all i and j satisfying $i \neq j$, we have $\pm \mathbf{x}_i$ not parallel to $\pm \mathbf{x}_j$, then Assumption 1 is satisfied. The validity of this assertion can be established by referring to [9, Theorem 3.1] for the proof.

Theorem 1 Suppose Assumption 1 holds, denote

$$\lambda_{a,p} := \lambda_{\min}(\mathbf{K}_p^{[a]}), \quad \lambda_{\omega,p} := \lambda_{\min}(\mathbf{K}_p^{[\omega]}).$$

Then we have $\lambda_{\omega,p+1} \geq \lambda_{\omega,p} > 0$, $\lambda_{a,p+1} \geq \lambda_{a,p} > 0$ for all $0 \leq s_p \leq s_{p+1}$.

Before the proof, we need a lemma in the linear algebra.

Lemma 1 (Weyl's Inequalities) Suppose \mathbf{A} and \mathbf{B} are real symmetric matrices, we have that

$$\lambda_{\min}(\mathbf{A} + \mathbf{B}) \geq \lambda_{\min}(\mathbf{A}) + \lambda_{\min}(\mathbf{B}). \quad (11)$$

Proof (Proof of Theorem 1) For the case $s_p < 1$, let's start by considering the expression for the matrix $\mathbf{K}_p^{[\omega]}$ where

$$\mathbf{K}_p^{[\omega]} = (K_{ij,p}^{[\omega]})_{n \times n} = \left(\mathbf{E}_{(a,\omega)} a^2 \sigma'_{s_p}(\boldsymbol{\omega}^T \mathbf{x}_i) \sigma'_{s_p}(\boldsymbol{\omega}^T \mathbf{x}_j) \mathbf{x}_i \cdot \mathbf{x}_j \right)_{n \times n}. \quad (12)$$

Given the derivative of the activation function:

$$\sigma'_{s_p}(x) = \begin{cases} 1, & x > 0 \\ (1 - s_p), & x < 0 \\ 0, & x = 0 \end{cases} \quad \sigma'_{s_{p+1}}(x) = \begin{cases} 1, & x > 0 \\ (1 - s_{p+1}), & x < 0 \\ 0, & x = 0 \end{cases}$$

we have

$$\sigma'_{s_{p+1}}(x) = \sigma'_{s_p}(x) + (s_p - s_{p+1})\sigma(-x) \quad (13)$$

$$\begin{aligned} & \mathbf{E}_{(a,\omega)} a^2 \sigma'_{s_{p+1}}(\omega^\top \mathbf{x}_i) \sigma'_{s_{p+1}}(\omega^\top \mathbf{x}_j) \mathbf{x}_i \cdot \mathbf{x}_j \\ = & \mathbf{E}_{(a,\omega)} a^2 \sigma'_{s_p}(\omega^\top \mathbf{x}_i) \sigma'_{s_p}(\omega^\top \mathbf{x}_j) \mathbf{x}_i \cdot \mathbf{x}_j \\ & - (s_p - s_{p+1}) \mathbf{E}_{(a,\omega)} a^2 [\sigma'(\omega^\top \cdot (-\mathbf{x}_i)) \sigma'_{s_p}(\omega^\top \mathbf{x}_j) (-\mathbf{x}_i) \cdot \mathbf{x}_j \\ & + \sigma'_{s_p}(\omega^\top \mathbf{x}_i) \sigma'(\omega^\top \cdot (-\mathbf{x}_j)) \mathbf{x}_i \cdot (-\mathbf{x}_j)] \\ & + (s_p - s_{p+1})^2 \mathbf{E}_{(a,\omega)} a^2 \sigma'(\omega^\top \cdot (-\mathbf{x}_i)) \sigma'(\omega^\top \cdot (-\mathbf{x}_j)) \mathbf{x}_i \cdot \mathbf{x}_j. \end{aligned} \quad (14)$$

Furthermore, since

$$\sigma'(x) = \frac{\sigma'_{s_p}(x) - s_p \sigma'_{s_p}(-x)}{1 - s_p^2}, \quad (15)$$

we have

$$\begin{aligned} & \sigma'(\omega^\top \cdot (-\mathbf{x}_i)) \sigma'_{s_p}(\omega^\top \mathbf{x}_j) (-\mathbf{x}_i) \cdot \mathbf{x}_j \\ = & \frac{1}{1 - s_p^2} \left[\sigma'_{s_p}(\omega^\top (-\mathbf{x}_i)) \sigma'_{s_p}(\omega^\top \mathbf{x}_j) (-\mathbf{x}_i) \mathbf{x}_j + s_p \sigma'_{s_p}(\omega^\top \mathbf{x}_i) \sigma'_{s_p}(\omega^\top \mathbf{x}_j) \mathbf{x}_i \mathbf{x}_j \right] \\ & \sigma'_{s_p}(\omega^\top \mathbf{x}_i) \sigma'(\omega^\top (-\mathbf{x}_j)) \mathbf{x}_i \cdot (-\mathbf{x}_j) \\ = & \frac{1}{1 - s_p^2} \left[\sigma'_{s_p}(\omega^\top \mathbf{x}_i) \sigma'_{s_p}(\omega^\top (-\mathbf{x}_j)) (-\mathbf{x}_i) \mathbf{x}_j + s_p \sigma'_{s_p}(\omega^\top \mathbf{x}_i) \sigma'_{s_p}(\omega^\top \mathbf{x}_j) \mathbf{x}_i \mathbf{x}_j \right]. \end{aligned} \quad (16)$$

Therefore,

$$\mathbf{K}_{p+1}^{[\omega]} = \left(1 + \frac{2s_p(s_{p+1} - s_p)}{1 - s_p^2} \right) \mathbf{K}_p^{[\omega]} + \frac{s_{p+1} - s_p}{1 - s_p^2} (\mathbf{M}_p^{[\omega]} + \mathbf{H}_p^{[\omega]}) + (s_{p+1} - s_p)^2 \mathbf{T}_M^{[\omega]}. \quad (17)$$

When $s_p < 1$, with the initial condition $s_0 = 0$, we can establish the following inequalities based on Assumption 1, where $\mathbf{K}_0^{[\omega]}$, $\mathbf{M}_0^{[\omega]}$, $\mathbf{H}_0^{[\omega]}$ is positive, and Lemma 1 holds:

$$\lambda_{\min}(\mathbf{K}_1^{[\omega]}) \geq 0. \quad (18)$$

The reason why $\mathbf{K}_0^{[\omega]}$, $\mathbf{M}_0^{[\omega]}$, $\mathbf{H}_0^{[\omega]}$ are positive definite matrices is indeed attributed to the fact that $\sigma'_0(x)$ is a constant function. Specifically, for $\mathbf{K}_0^{[\omega]}$, it can be represented as

$$(a(\mathbf{x}_1, \mathbf{x}_2, \dots, \mathbf{x}_n))^T \cdot a(\mathbf{x}_1, \mathbf{x}_2, \dots, \mathbf{x}_n),$$

which is inherently positive definite. Similar propositions can be derived for $\mathbf{M}_0^{[\omega]}$ and $\mathbf{H}_0^{[\omega]}$ based on the same principle.

Now, when $0 \leq s_p \leq s_{p+1}$ and $s_p < 1$ and Lemma 1 holds:

$$\lambda_{\min}(\mathbf{K}_{p+1}^{[\omega]}) \geq \lambda_{\min}(\mathbf{K}_p^{[\omega]}) \geq 0$$

due to Eqs. (17,18).

For the case $s_p \geq 1$, we have that

$$\begin{aligned}
& \mathbf{E}_{(a,\omega)} a^2 \sigma'_{s_{p+1}}(\omega^\top \mathbf{x}_i) \sigma'_{s_{p+1}}(\omega^\top \mathbf{x}_j) \mathbf{x}_i \cdot \mathbf{x}_j \\
&= \mathbf{E}_{(a,\omega)} a^2 \sigma'_{s_p}(\omega^\top \mathbf{x}_i) \sigma'_{s_p}(\omega^\top \mathbf{x}_j) \mathbf{x}_i \cdot \mathbf{x}_j \\
&\quad - (s_p - s_{p+1}) \mathbf{E}_{(a,\omega)} a^2 [\sigma'(\omega^\top \cdot (-\mathbf{x}_i)) \sigma'_{s_p}(\omega^\top \mathbf{x}_j) (-\mathbf{x}_i) \cdot \mathbf{x}_j \\
&\quad + \sigma'_{s_p}(\omega^\top \mathbf{x}_i) \sigma'(\omega^\top \cdot (-\mathbf{x}_j)) \mathbf{x}_i \cdot (-\mathbf{x}_j)] \\
&\quad + (s_p - s_{p+1})^2 \mathbf{E}_{(a,\omega)} a^2 \sigma'(\omega^\top \cdot (-\mathbf{x}_i)) \sigma'(\omega^\top \cdot (-\mathbf{x}_j)) \mathbf{x}_i \cdot \mathbf{x}_j. \tag{19}
\end{aligned}$$

Furthermore, since

$$\sigma'_{s_p}(x) = \sigma'(x) + (1 - s_p) \sigma'(-x), \tag{20}$$

we have

$$\begin{aligned}
& \sigma'(\omega^\top \cdot (-\mathbf{x}_i)) \sigma'_{s_p}(\omega^\top \mathbf{x}_j) (-\mathbf{x}_i) \cdot \mathbf{x}_j \\
&= \sigma'(\omega^\top \cdot (-\mathbf{x}_i)) \sigma'(\omega^\top \mathbf{x}_j) (-\mathbf{x}_i) \cdot \mathbf{x}_j - (1 - s_p) \sigma'(\omega^\top (-\mathbf{x}_i)) \sigma'(\omega^\top (-\mathbf{x}_j)) (-\mathbf{x}_i) (-\mathbf{x}_j) \\
&\quad + \sigma'_{s_p}(\omega^\top \mathbf{x}_i) \sigma'(\omega^\top (-\mathbf{x}_j)) \mathbf{x}_i \cdot (-\mathbf{x}_j) \\
&= \sigma'(\omega^\top \cdot \mathbf{x}_i) \sigma'(\omega^\top (-\mathbf{x}_j)) (-\mathbf{x}_i) \cdot \mathbf{x}_j - (1 - s_p) \sigma'(\omega^\top (-\mathbf{x}_i)) \sigma'(\omega^\top (-\mathbf{x}_j)) (-\mathbf{x}_i) (-\mathbf{x}_j).
\end{aligned}$$

Therefore,

$$\mathbf{K}_{p+1}^{[\omega]} = \mathbf{K}_p^{[\omega]} - (1 - s_p)(s_{p+1} - s_p)(\mathbf{M}_M^{[\omega]} + \mathbf{H}_M^{[\omega]}) + (s_{p+1} - s_p)(s_{p+1} - s_p + 2) \mathbf{T}_M^{[\omega]}.$$

When $0 \leq s_p \leq s_{p+1}$ and $s_p \geq 1$, we have that

$$\lambda_{\min}(\mathbf{K}_{p+1}^{[\omega]}) \geq \lambda_{\min}(\mathbf{K}_p^{[\omega]}) \geq 0$$

based on Assumption 1, as well as Lemma 1. Similar results can be derived for the Gram matrices with respect to the parameter a .

3.3 Convergence of t_1 iteration

The convergence of the first iteration aligns with the traditional neural target kernel analysis. For brevity, we omit the proof in this subsection; however, readers can find comprehensive details in [20, 11, 30]. Here, we introduce the three results that will be employed in the subsequent iterations.

Lemma 2 (bounds of initial parameters [30]) *Given $\delta \in (0, 1)$, we have with probability at least $1 - \delta$ over the choice of $\boldsymbol{\theta}(0)$ such that*

$$\max_{k \in [m]} \{|a_k(0)|, \|\boldsymbol{\omega}_k(0)\|_\infty\} \leq \sqrt{2 \log \frac{2m(d+1)}{\delta}}. \tag{21}$$

Proposition 1 ([30]) *Given the sample set $S = \{(\mathbf{x}_i, y_i)\}_{i=1}^n \subset \Omega$ with \mathbf{x}_i 's drawn i.i.d. with uniformly distributed and $\delta \in (0, 1)$. Suppose that Assumption 1 holds. If $m \geq \frac{16n^2 d^2 C_{\psi, d}}{C_0 \lambda^2} \log \frac{4n^2}{\delta}$ then with probability at least $1 - \delta$ over the choice of $\boldsymbol{\theta}(0)$, we have*

$$\lambda_{\min}(\mathbf{G}_1(\boldsymbol{\theta}(0))) \geq \frac{3}{4}(\lambda_{a,1} + \lambda_{\omega,1}),$$

where C_0 is an absolute constant shown in Proposition 6.

Set

$$t_1^* = \inf\{t \mid \boldsymbol{\theta}(t) \notin \mathcal{N}_1(\boldsymbol{\theta}(0))\} \quad (22)$$

where

$$\mathcal{N}_1(\boldsymbol{\theta}(0)) := \left\{ \boldsymbol{\theta} \mid \|\mathbf{G}_2(\boldsymbol{\theta}) - \mathbf{G}_1(\boldsymbol{\theta}(0))\|_F \leq \frac{1}{4}(\lambda_{a,1} + \lambda_{\omega,1}) \right\}.$$

Note that t_1^* represents the maximum time parameter, ensuring that the smallest eigenvalue of the dynamic is not small and positive. This condition facilitates an exponential decay of the loss functions. Outside this designated region, the rate of decay might decelerate, making it challenging to achieve rapid convergence.

The principle behind the homotopy approach involves modifying the activation functions to alter the energy landscape of the loss functions. This adjustment aims to ensure that the smallest eigenvalue remains large and positive. The rationale for this modification stems from the concept of $\boldsymbol{\theta}$ -lazy training in the neural target kernel and the corresponding increase in the smallest eigenvalue (Theorem 1). Further details on this topic will be elaborated upon in subsequent sections.

Proposition 2 ([30]) *Given the sample set $S = \{(\mathbf{x}_i, y_i)\}_{i=1}^n \subset \Omega$ with \mathbf{x}_i 's drawn i.i.d. with uniformly distributed and $\delta \in (0, 1)$. Suppose that Assumption 1 holds. If $m \geq \frac{16n^2 d^2 C_{\psi, d}}{C_0 \lambda^2} \log \frac{4n^2}{\delta}$ then with probability at least $1 - \delta$ over the choice of $\boldsymbol{\theta}(0)$, we have for any $t \in [0, t_1^*]$*

$$\mathcal{R}_{S, s_1}(\boldsymbol{\theta}(t)) \leq \mathcal{R}_{S, s_1}(\boldsymbol{\theta}(0)) \exp\left(-\frac{t}{n}(\lambda_{a,1} + \lambda_{\omega,1})\right), \quad (23)$$

where C_0 is an absolute constant shown in Proposition 6.

3.4 Convergence of t_2 iteration

In this paper, without sacrificing generality, we focus our attention on the case where $M = 2$. However, it's important to note that our analysis and methodology can readily be extended to the broader scenario of $M \geq 2$.

The following method presents the $\boldsymbol{\theta}$ -lazy training. This proposition is crucial, as if $\boldsymbol{\theta}(t_1^*)$ deviates significantly from the initial value, even with the

smallest eigenvalue of the dynamical system increasing during the homotopy and relaxation training, the gap may cause the dynamical system at the beginning of the second iteration, i.e., the end of the first iteration, to be not positive.

Proposition 3 ([30]) *Given the sample set $S = \{(\mathbf{x}_i, y_i)\}_{i=1}^n \subset \Omega$ with \mathbf{x}_i 's drawn i.i.d. with uniformly distributed and $\delta \in (0, 1)$. Suppose that Assumption 1 holds. If*

$$m \geq \max \left\{ \frac{16n^2 d^2 C_{\psi, d}}{C_0 \lambda^2} \log \frac{4n^2}{\delta}, \frac{8n^2 d^2 \mathcal{R}_{S, s_1}(\boldsymbol{\theta}(0))}{(\lambda_{a,1} + \lambda_{\omega,1})^2} \right\}$$

then with probability at least $1 - \delta$ over the choice of $\boldsymbol{\theta}(0)$, we have for any $t \in [0, t_1^*]$

$$\begin{aligned} & \max_{k \in [m]} \{ |a_k(t) - a_k(0)|, \|\boldsymbol{\omega}_k(t) - \boldsymbol{\omega}_k(0)\|_\infty \} \\ & \leq \frac{8\sqrt{2}nd\sqrt{\mathcal{R}_{S, s_1}(\boldsymbol{\theta}(0))}}{\sqrt{m}(\lambda_{a,1} + \lambda_{\omega,1})} \sqrt{2 \log \frac{4m(d+1)}{\delta}}, \end{aligned}$$

where C_0 is an absolute constant shown in Proposition 6.

For simplicity, we define a $\mathcal{O}\left(\frac{\log m}{\sqrt{m}}\right)$ term ψ , which is

$$\psi(m) := \frac{8\sqrt{2}nd\sqrt{\mathcal{R}_{S, s_1}(\boldsymbol{\theta}(0))}}{(\lambda_{a,1} + \lambda_{\omega,1})} \sqrt{2 \log \frac{4m(d+1)}{\delta}}.$$

Moving forward, we will employ $\boldsymbol{\theta}(t_1^*)$ as the initial value for training over t_2 iterations. However, before we proceed, it is crucial to carefully select the value of s_2 . This choice of s_2 depends on both $\mathcal{R}_{S, s_1}(\boldsymbol{\theta}(t_1^*))$ and a constant ζ , with the condition that ζ is a positive constant, ensuring that $0 < \zeta$. Therefore, we define s_2 as: $s_2 = s_1 + \zeta$ where $\zeta > 0$ is a constant.

It's important to emphasize that for each $\boldsymbol{\theta}(t_1^*)$, given that the training dynamics system operates without any random elements, we can determine it once we know $\boldsymbol{\theta}(0)$. In other words, we can consider $\boldsymbol{\theta}(t_1^*)$ as two distinct functions, $\boldsymbol{\theta} = (\bar{a}, \boldsymbol{\omega})$, with $\boldsymbol{\theta}(0)$ as their input. This implies that $\bar{a}(\boldsymbol{\theta}(t_0)) = a(t_1^*)$ and $\bar{\boldsymbol{\omega}}(\boldsymbol{\theta}(0)) = \boldsymbol{\omega}(t_1^*)$.

Lemma 3 *Suppose that $\boldsymbol{\omega} := \boldsymbol{\omega}(0) \sim N(0, \mathbf{I}_d)$, $a = a(0) \sim N(0, 1)$ and given $\mathbf{x}_i, \mathbf{x}_j \in \Omega$. If*

$$m \geq \max \left\{ \frac{16n^2 d^2 C_{\psi, d}}{C_0 \lambda^2} \log \frac{4n^2}{\delta}, \frac{8n^2 d^2 \mathcal{R}_{S, s_1}(\boldsymbol{\theta}(0))}{(\lambda_{a,1} + \lambda_{\omega,1})^2} \right\}$$

then with probability at least $1 - \delta$ over the choice of $\boldsymbol{\theta}(0)$, we have

$$(i) \text{ if } \mathbf{X} := \sigma_{s_2}(\bar{\boldsymbol{\omega}}^\top(\boldsymbol{\omega})\mathbf{x}_i) \sigma_{s_2}(\bar{\boldsymbol{\omega}}^\top(\boldsymbol{\omega}) \cdot \mathbf{x}_j), \text{ then } \|\mathbf{X}\|_{\psi_1} \leq 2dC_{\psi, d} + \frac{2d^2\psi(m)^2}{\log 2}.$$

(ii) if $X := \bar{a}(a)^2 \sigma'_{s_2}(\bar{\omega}^\top(\omega)\mathbf{x}_i) \sigma'_{s_2}(\bar{\omega}^\top(\omega)\mathbf{x}_j) \mathbf{x}_i \cdot \mathbf{x}_j$, then $\|X\|_{\psi_1} \leq 2dC_{\psi,d} + \frac{2d^2\psi(m)^2}{\log 2}$, where

$$\|X\|_{\psi_1} := \inf\{s > 0 \mid \mathbf{E}_X[e^{|X|/s}] \leq 2\}, \quad (24)$$

$C_{\psi,d} := \|\chi^2(d)\|_{\psi_1}$ for $\chi^2(d)$ being the chi-square random variable in d -dimensional spaces, and where C_0 is an absolute constant shown in Proposition 6.

Proof (i)

$$|X| \leq d\|\bar{\omega}(\omega)\|_2^2 \leq 2d\|\omega\|_2^2 + 2d\|\bar{\omega}(\omega) - \omega\|_2^2 \leq 2d|Z| + 2d^2\psi(m)^2$$

where $|Z| := \|\omega\|_2^2$, and

$$\begin{aligned} \|X\|_{\psi_1} &= \inf\{s > 0 \mid \mathbf{E}_X \exp(|X|/s) \leq 2\} \\ &= \inf\{s > 0 \mid \mathbf{E}_\omega \exp(|\sigma_{s_2}(\bar{\omega}^\top(\omega)\mathbf{x}_i) \sigma_{s_2}(\bar{\omega}^\top(\omega) \cdot \mathbf{x}_j)|/s) \leq 2\} \\ &\leq \inf\left\{s > 0 \mid \mathbf{E}_\omega \exp\left(\frac{2d|Z| + 2d^2\psi(m)^2}{s}\right) \leq 2\right\} \\ &\leq \inf\{s > 0 \mid \mathbf{E}_Z \exp(2d|Z|/s) \leq 2\} + \inf\left\{s > 0 \mid \mathbf{E}_\omega \exp\left(\frac{2d^2\psi(m)^2}{s}\right) \leq 2\right\} \\ &= 2d\|\chi^2(d)\|_{\psi_1} + \frac{2d^2\psi(m)^2}{\log 2} \\ &\leq 2dC_{\psi,d} + \frac{2d^2\psi(m)^2}{\log 2}. \end{aligned}$$

(ii) $|X| \leq d|a|^2 \leq 2d|Z| + 2d^2\psi(m)^2$ and $\|X\|_{\psi_1} \leq 2dC_{\psi,d} + \frac{2d^2\psi(m)^2}{\log 2}$.

To enhance simplicity and maintain consistent notation, we define:

$$C_{\psi,d,2} := 2C_{\psi,d} + \frac{2d\psi(m)^2}{\log 2}. \quad (25)$$

Based on the above lemma and the sub-exponential Bernstein's inequality as outlined in [39] (which we demonstrate in the appendix), we can conclude that the smallest eigenvalue at the beginning of the second iteration remains positive.

Proposition 4 Given $\delta \in (0, 1)$ and the sample set $S = \{(\mathbf{x}_i, y_i)\}_{i=1}^n$ with \mathbf{x}_i 's drawn i.i.d. with uniformly distributed. Suppose that Assumption 1 holds. If

$$m \geq \max\left\{\frac{16n^2 d^2 C_{\psi,d}}{C_0 \lambda^2} \log \frac{4n^2}{\delta}, n^4 \left(\frac{256\sqrt{2}d\sqrt{\mathcal{R}_{S,S_1}(\boldsymbol{\theta}(0))}}{(\lambda_{a,1} + \lambda_{\omega,1}) \min\{\lambda_{a,2}, \lambda_{\omega,2}\}} \log \frac{4m(d+1)}{\delta}\right)\right\}$$

then with probability at least $1 - \delta$ over the choice of $\boldsymbol{\theta}(0)$, we have

$$\lambda_{\min}(\mathbf{G}_2(\boldsymbol{\theta}(t_1^*))) \geq \frac{3}{4}(\lambda_{a,2} + \lambda_{2,\omega}),$$

where C_0 is an absolute constant shown in Proposition 6.

Proof

$$\begin{aligned}\bar{k}_2^{[a]}(\mathbf{x}, \mathbf{x}') &:= \mathbf{E}_{\omega} \sigma_{s_2}(\bar{\omega}^\top(\omega)\mathbf{x}) \sigma_{s_2}(\bar{\omega}^\top(\omega) \cdot \mathbf{x}') \\ \bar{k}_2^{[\omega]}(\mathbf{x}, \mathbf{x}') &:= \mathbf{E}_{(a,\omega)} \bar{a}(a)^2 \sigma'_{s_2}(\bar{\omega}^\top(\omega)\mathbf{x}) \sigma'_{s_2}(\bar{\omega}^\top(\omega)\mathbf{x}') \mathbf{x} \cdot \mathbf{x}'.\end{aligned}\quad (26)$$

The Gram matrices, denoted as $\bar{\mathbf{K}}_2^{[a]}$ and $\bar{\mathbf{K}}_2^{[\omega]}$, corresponding to an infinite-width two-layer network with the activation function σ_{s_2} , can be expressed as follows:

$$\begin{aligned}\bar{K}_{ij,2}^{[a]} &= \bar{k}_2^{[a]}(\mathbf{x}_i, \mathbf{x}_j), \quad \bar{\mathbf{K}}_2^{[a]} = (\bar{K}_{ij,2}^{[a]})_{n \times n}, \\ \bar{K}_{ij,2}^{[\omega]} &= \bar{k}_2^{[\omega]}(\mathbf{x}_i, \mathbf{x}_j), \quad \bar{\mathbf{K}}_2^{[\omega]} = (\bar{K}_{ij,2}^{[\omega]})_{n \times n}.\end{aligned}\quad (27)$$

The proof can be divided into two main parts. The first part, seeks to establish that the difference between $\mathbf{K}_2^{[a]} + \mathbf{K}_2^{[\omega]}$ and $\bar{\mathbf{K}}_2^{[a]} + \bar{\mathbf{K}}_2^{[\omega]}$ is small. In this case, the proof draws upon Proposition 3, which underscores the potential for the error in $\|\boldsymbol{\theta}(0) - \boldsymbol{\theta}(t^*)\|_\infty$ to be highly negligible when m assumes a large value. The second part aims to demonstrate that the disparity between $\mathbf{G}(\boldsymbol{\theta}(t_1^*))$ and $\bar{\mathbf{K}}_2^{[a]} + \bar{\mathbf{K}}_2^{[\omega]}$ is minimal. This particular proof relies on the application of sub-exponential Bernstein's inequality as outlined in [39] (Proposition 6).

First of all, we prove that the difference between $\mathbf{K}_2^{[a]} + \mathbf{K}_2^{[\omega]}$ and $\bar{\mathbf{K}}_2^{[a]} + \bar{\mathbf{K}}_2^{[\omega]}$ is small. Due to

$$\begin{aligned}\left| \bar{k}_2^{[a]}(\mathbf{x}, \mathbf{x}') - k_2^{[a]}(\mathbf{x}, \mathbf{x}') \right| &\leq \mathbf{E}_{\omega} \left| \sigma_{s_2}(\bar{\omega}^\top(\omega)\mathbf{x}) \sigma_{s_2}(\bar{\omega}^\top(\omega)\mathbf{x}') - \sigma_{s_2}(\omega\mathbf{x}) \sigma_{s_2}(\omega \cdot \mathbf{x}') \right| \\ &\leq 2d \|\bar{\omega}^\top(\omega(0)) - \omega(0)\|_\infty \|\omega(0)\|_\infty \\ &\leq 2d\psi(m) \sqrt{2 \log \frac{4m(d+1)}{\delta}}\end{aligned}\quad (28)$$

with probability at least $1 - \delta$ over the choice of $\boldsymbol{\theta}(0)$, where the last inequality is due to Lemma 2. Therefore,

$$\|\mathbf{K}_2^{[a]} - \bar{\mathbf{K}}_2^{[a]}\|_F \leq 2n\psi(m) \sqrt{2 \log \frac{4m(d+1)}{\delta}}.\quad (29)$$

Similarly, we can obtain that

$$\|\mathbf{K}_2^{[\omega]} - \bar{\mathbf{K}}_2^{[\omega]}\|_F \leq 2n\psi(m) \sqrt{2 \log \frac{4m(d+1)}{\delta}}.\quad (30)$$

Set $\psi(m) \leq \frac{\min\{\lambda_{a,2}, \lambda_{\omega,2}\}}{16n \sqrt{2 \log \frac{4m(d+1)}{\delta}}}$, i.e.

$$m \geq n^4 \left(\frac{128\sqrt{2}d\sqrt{\mathcal{R}_{S,s_1}(\boldsymbol{\theta}(0))}}{(\lambda_{a,1} + \lambda_{\omega,1}) \min\{\lambda_{a,2}, \lambda_{\omega,2}\}} 2 \log \frac{4m(d+1)}{\delta} \right),$$

we have

$$\max\{\|\mathbf{K}_2^{[a]} - \bar{\mathbf{K}}_2^{[a]}\|_F, \|\mathbf{K}_2^{[\omega]} - \bar{\mathbf{K}}_2^{[\omega]}\|_F\} \leq \frac{1}{8} \min\{\lambda_{a,2}, \lambda_{\omega,2}\}.$$

Furthermore, by sub-exponential Bernstein's inequality as outlined in [39] (Proposition 6), for any $\varepsilon > 0$, we define

$$\begin{aligned} \mathbb{A}_{ij,2}^{[a]} &:= \left\{ \boldsymbol{\theta}(0) \mid \left| G_{ij,2}^{[a]}(\boldsymbol{\theta}(0)) - \bar{K}_{ij,2}^{[a]} \right| \leq \frac{\varepsilon}{n} \right\} \\ \mathbb{A}_{ij,2}^{[\omega]} &:= \left\{ \boldsymbol{\theta}(0) \mid \left| G_{ij,2}^{[\omega]}(\boldsymbol{\theta}(0)) - \bar{K}_{ij,2}^{[\omega]} \right| \leq \frac{\varepsilon}{n} \right\}. \end{aligned} \quad (31)$$

Setting $\varepsilon \leq ndC_{\psi,d,2}$, by Proposition 6 and Lemma 4, we have

$$\begin{aligned} \mathbf{P}(\mathbb{A}_{ij,2}^{[a]}) &\geq 1 - 2 \exp\left(-\frac{mC_0\varepsilon^2}{n^2d^2C_{\psi,d,2}}\right), \\ \mathbf{P}(\mathbb{A}_{ij,2}^{[\omega]}) &\geq 1 - 2 \exp\left(-\frac{mC_0\varepsilon^2}{n^2d^2C_{\psi,d,2}}\right). \end{aligned} \quad (32)$$

Therefore, with probability at least

$$\left[1 - 2 \exp\left(-\frac{mC_0\varepsilon^2}{n^2d^2C_{\psi,d,2}^2}\right) \right]^{2n^2} \geq 1 - 4n^2 \exp\left(-\frac{mC_0\varepsilon^2}{n^2d^2C_{\psi,d,2}^2}\right)$$

over the choice of $\boldsymbol{\theta}(0)$, we have

$$\begin{aligned} \left\| G_2^{[a]}(\boldsymbol{\theta}(0)) - \bar{K}_2^{[a]} \right\|_F &\leq \varepsilon \\ \left\| G_2^{[\omega]}(\boldsymbol{\theta}(0)) - \bar{K}_2^{[\omega]} \right\|_F &\leq \varepsilon. \end{aligned} \quad (33)$$

Hence by taking $\varepsilon = \frac{1}{8} \min\{\lambda_{a,2}, \lambda_{\omega,2}\}$ and $\delta = 4n^2 \exp\left(-\frac{mC_0\lambda_1^2}{16n^2d^2C_{\psi,d,2}^2}\right)$, we obtain that

$$\begin{aligned} \lambda_{\min}(\mathbf{G}_2(\boldsymbol{\theta}(t_1^*))) &\geq \lambda_{\min}(\mathbf{G}_2^{[a]}(\boldsymbol{\theta}(t_1^*))) + \lambda_{\min}(\mathbf{G}_2^{[\omega]}(\boldsymbol{\theta}(t_1^*))) \\ &\geq \lambda_{a,1} + \lambda_{\omega,1} - \left\| \mathbf{G}_2^{[a]}(\boldsymbol{\theta}(t_1^*)) - \bar{\mathbf{K}}_2^{[a]} \right\|_F - \left\| \mathbf{G}_2^{[\omega]}(\boldsymbol{\theta}(t_1^*)) - \bar{\mathbf{K}}_2^{[\omega]} \right\|_F \\ &\quad - \left\| \mathbf{K}_2^{[a]} - \bar{\mathbf{K}}_2^{[a]} \right\|_F - \left\| \mathbf{K}_2^{[\omega]} - \bar{\mathbf{K}}_2^{[\omega]} \right\|_F \\ &\geq \frac{3}{4}(\lambda_{a,2} + \lambda_{\omega,2}). \end{aligned} \quad (34)$$

Remark 3 In accordance with Proposition 4, we can establish that m follows a trend of $\mathcal{O}\left(\frac{\log(1/\delta)}{\min\{\lambda_{a,2}, \lambda_{\omega,2}\}}\right)$. This observation sheds light on our strategy of increasing the parameter s with each iteration. As we have proven in Theorem 1, the smallest eigenvalues of Gram matrices tend to increase as s increases. This insight provides a reason for increasing the activation parameters, thereby enhancing the probability that the Gram matrix is positive and making the

energy landscape in this iteration more convex. Now, consider the second iteration. For a fixed value of m that we have at this stage, a larger smallest eigenvalue implies that we can select a smaller value for δ . Consequently, this leads to a higher probability of $\lambda_{\min}(\mathbf{G}_2(\boldsymbol{\theta}(t_1^*)))$ being positive.

If we maintain the activation function unchanged and proceed with the proof of Proposition 4, it can be inferred that the dynamics at the onset of the second iteration are positive if m satisfies

$$C \frac{\log(1/\delta)}{\min\{\lambda_{a,2}, \lambda_{\omega,2}\}} \leq m \leq C \frac{\log(1/\delta)}{\min\{\lambda_{a,1}, \lambda_{\omega,1}\}},$$

where C is a constant. However, this positivity guarantee would not hold if the activation functions remain unchanged.

Set

$$t_2^* = \inf\{t \mid \boldsymbol{\theta}(t) \notin \mathcal{N}_2(\boldsymbol{\theta}(t_1^*))\} \quad (35)$$

where

$$\mathcal{N}_2(\boldsymbol{\theta}(t_1^*)) := \left\{ \boldsymbol{\theta} \mid \|\mathbf{G}_2(\boldsymbol{\theta}) - \mathbf{G}_2(\boldsymbol{\theta}(t_1^*))\|_F \leq \frac{1}{4}(\lambda_{a,2} + \lambda_{\omega,2}) \right\}.$$

Proposition 5 *Given the sample set $S = \{(\mathbf{x}_i, y_i)\}_{i=1}^n \subset \Omega$ with \mathbf{x}_i 's drawn i.i.d. with uniformly distributed and $\delta \in (0, 1)$. Suppose that Assumption 1 holds.*

$$m \geq \max \left\{ \frac{16n^2 d^2 C_{\psi,d}}{C_0 \lambda^2} \log \frac{4n^2}{\delta}, n^4 \left(\frac{256\sqrt{2}d\sqrt{\mathcal{R}_{S,s_1}(\boldsymbol{\theta}(0))}}{(\lambda_{a,1} + \lambda_{\omega,1}) \min\{\lambda_{a,2}, \lambda_{\omega,2}\}} \log \frac{4m(d+1)}{\delta} \right) \right\}$$

then with probability at least $1 - \delta$ over the choice of $\boldsymbol{\theta}(0)$, we have for any $t \in [t_1^*, t_2^*]$

$$\mathcal{R}_{S,s_2}(\boldsymbol{\theta}(t)) \leq \mathcal{R}_{S,s_2}(\boldsymbol{\theta}(t_1^*)) \exp\left(-\frac{t-t_1^*}{n}(\lambda_{a,2} + \lambda_{\omega,2})\right), \quad (36)$$

where C_0 is an absolute constant shown in Proposition 6.

Proof Due to Proposition 4 and the definition of t_2^* , we have that for any $\delta \in (0, 1)$

$$\lambda_{\min}(\mathbf{G}_2(\boldsymbol{\theta}(t))) \geq \frac{1}{2}(\lambda_{a,1} + \lambda_{\omega,1}) \quad (37)$$

for any $t \in [t_1^*, t_2^*]$ with probability at least $1 - \delta$ over the choice of $\boldsymbol{\theta}(0)$.

Then we get that

$$\begin{aligned} \frac{d}{dt} \mathcal{R}_{S,s_2}(\boldsymbol{\theta}(t)) &= \sum_{k=1}^m \left(\nabla_{a_k} \mathcal{R}_{S,s_2}(\boldsymbol{\theta}) \frac{da_k(t)}{dt} + \nabla_{\omega_k} \mathcal{R}_{S,s_2}(\boldsymbol{\theta}) \frac{d\omega_k(t)}{dt} \right) \\ &= -\frac{1}{n^2} \mathbf{e}_2^T \mathbf{G}_2(\boldsymbol{\theta}(t)) \mathbf{e}_2 \\ &\leq -\frac{2}{n} \lambda_{\min}(\mathbf{G}_2(\boldsymbol{\theta})) \mathcal{R}_{S,s_2}(\boldsymbol{\theta}(t)) \\ &\leq -\frac{1}{n} (\lambda_{a,2} + \lambda_{\omega,2}) \mathcal{R}_{S,s_2}(\boldsymbol{\theta}(t)). \end{aligned} \quad (38)$$

Therefore,

$$\mathcal{R}_{S,s_2}(\boldsymbol{\theta}(t)) \leq \mathcal{R}_{S,s_2}(\boldsymbol{\theta}(t_1^*)) \exp\left(-\frac{t-t_1^*}{n}(\lambda_{a,2} + \lambda_{\omega,2})\right). \quad (39)$$

3.5 Convergence of HRTA

By combining Propositions 2 and 5, we can establish the convergence of the HRTA.

Theorem 2 *Given $\delta \in (0, 1)$, $s_1 \in (0, +\infty)$, $\zeta > 1$ and the sample set $S = \{(\mathbf{x}_i, y_i)\}_{i=1}^n$ with \mathbf{x}_i 's drawn i.i.d. with uniformly distributed. Suppose that Assumption 1 holds,*

$$m \geq \max \left\{ \frac{16n^2 d^2 C_{\psi,d}}{C_0 \lambda^2} \log \frac{4n^2}{\delta}, n^4 \left(\frac{256\sqrt{2}d\sqrt{\mathcal{R}_{S,s_1}(\boldsymbol{\theta}(0))}}{(\lambda_{a,1} + \lambda_{\omega,1}) \min\{\lambda_{a,2}, \lambda_{\omega,2}\}} \log \frac{4m(d+1)}{\delta} \right) \right\}$$

then with probability at least $1 - \delta$ over the choice of $\boldsymbol{\theta}(0)$, we have

$$\begin{cases} \mathcal{R}_{S,s_1}(\boldsymbol{\theta}(t)) \leq \mathcal{R}_{S,s_1}(\boldsymbol{\theta}(0)) \exp\left(-\frac{t}{n}(\lambda_{a,1} + \lambda_{\omega,1})\right), t \in [0, t_1^*] \\ \mathcal{R}_{S,s_2}(\boldsymbol{\theta}(t)) \leq \mathcal{R}_{S,s_2}(\boldsymbol{\theta}(t_1^*)) \exp\left(-\frac{t-t_1^*}{n}(\lambda_{a,2} + \lambda_{\omega,2})\right), t \in [t_1^*, t_2^*]. \end{cases}$$

where t_i^* are defined in Eqs. (22, 35). Furthermore, we have that the decay speed in $[t_1^*, t_2^*]$ can be faster than $[0, t_1^*]$, i.e.

$$\begin{aligned} \mathcal{R}_{S,s_2}(\boldsymbol{\theta}(t)) &\leq \mathcal{R}_{S,s_2}(\boldsymbol{\theta}(t_1^*)) \exp\left(-\frac{t-t_1^*}{n}(\lambda_{a,2} + \lambda_{\omega,2})\right) \\ &\leq \mathcal{R}_{S,s_2}(\boldsymbol{\theta}(t_1^*)) \exp\left(-\frac{t-t_1^*}{n}(\lambda_{a,1} + \lambda_{\omega,1})\right), \end{aligned} \quad (40)$$

where C_0 is an absolute constant shown in Proposition 6.

Proof By amalgamating Propositions 2 and 5, we can readily derive the proof for Theorem 2.

Corollary 1 *Given $\delta \in (0, 1)$, $s_1 \in (0, +\infty)$, $\zeta > 1$ and the sample set $S = \{(\mathbf{x}_i, y_i)\}_{i=1}^n$ with \mathbf{x}_i 's drawn i.i.d. with uniformly distributed. Suppose that Assumption 1 holds,*

$$m \geq \max \left\{ \frac{16n^2 d^2 C_{\psi,d}}{C_0 \lambda^2} \log \frac{4n^2}{\delta}, n^4 \left(\frac{256\sqrt{2}d\sqrt{\mathcal{R}_{S,s_1}(\boldsymbol{\theta}(0))}}{(\lambda_{a,1} + \lambda_{\omega,1}) \min\{\lambda_{a,2}, \lambda_{\omega,2}\}} \log \frac{4m(d+1)}{\delta} \right) \right\}$$

and $s_2 := \inf \{s \in (s_1, 2) \mid \mathcal{R}_{S,s}(\boldsymbol{\theta}(t_1^*)) > \zeta \mathcal{R}_{S,s_1}(\boldsymbol{\theta}(t_1^*))\}$, then with probability at least $1 - \delta$ over the choice of $\boldsymbol{\theta}(0)$, we have for any $t \in [t_1^*, t_2^*]$

$$\mathcal{R}_{S,s_2}(\boldsymbol{\theta}(t)) \leq \zeta \mathcal{R}_{S,s_1}(\boldsymbol{\theta}(0)) \exp\left(-\frac{t_1^*}{n}(\lambda_{a,1} + \lambda_{\omega,1})\right) \exp\left(-\frac{t-t_1^*}{n}(\lambda_{a,2} + \lambda_{\omega,2})\right). \quad (41)$$

Remark 4 In the case where $M \geq 2$, note that we may consider the scenario where m becomes larger. However, it's important to emphasize that the order of m remains at $\mathcal{O}(n^4)$. This order does not increase substantially due to the fact that all the derivations presented in Subsection 3.4 can be smoothly generalized.

Building upon the proof of Theorem 2, we can recognize the advantages of the HRTA. In the initial iteration, the training process does not differ significantly from training using training for pure ReLU networks. The traditional method can effectively reduce the loss function within the set $\mathcal{N}_1(\boldsymbol{\theta}(0))$, defined as:

$$\mathcal{N}_1(\boldsymbol{\theta}(0)) := \left\{ \boldsymbol{\theta} \mid \|\mathbf{G}_1(\boldsymbol{\theta}) - \mathbf{G}_1(\boldsymbol{\theta}(0))\|_F \leq \frac{1}{4}(\lambda_{a,1} + \lambda_{\omega,1}) \right\}.$$

In other words, the traditional method can effectively minimize the loss function within the time interval $[0, t_1^*]$, where $t_1^* = \inf\{t \mid \boldsymbol{\theta}(t) \notin \mathcal{N}_1(\boldsymbol{\theta}(0))\}$. Outside of this range, the training speed may slow down significantly and take a long time to converge. However, the HRTA transits the training dynamics to a new kernel by introducing a new activation function. This allows training to converge efficiently within a new range of $\boldsymbol{\theta}$, defined as:

$$\mathcal{N}_2(\boldsymbol{\theta}(t_1^*)) := \left\{ \boldsymbol{\theta} \mid \|\mathbf{G}_2(\boldsymbol{\theta}) - \mathbf{G}_2(\boldsymbol{\theta}(t_1^*))\|_F \leq \frac{1}{4}(\lambda_{a,2} + \lambda_{\omega,2}) \right\},$$

if $\mathbf{G}_2(\boldsymbol{\theta}(t_1^*))$ is strictly positive definite. Furthermore, we demonstrate that the minimum eigenvalue of $\mathbf{G}_2(\boldsymbol{\theta}(t_1^*))$ surpasses that of $\mathbf{G}_1(\boldsymbol{\theta}(0))$ under these conditions, as indicated by Theorem 1. This implies that, rather than decaying, the training speed may actually increase. This is one of the important reasons why we believe that relaxation surpasses traditional training methods in neural network training. Furthermore, in this paper, we provide evidence that $\mathbf{G}_2(\boldsymbol{\theta}(t_1^*))$ indeed becomes strictly positive definite when the width of neural networks is sufficiently large. Building upon Proposition 4, we can see that the increasing smallest eigenvalue of Gram matrices in each iteration contributes to a higher likelihood of $\mathbf{G}_2(\boldsymbol{\theta}(t_1^*))$ becoming strictly positive definite.

As the number of iterations increases, the algorithm may not always be effective. On one hand, the time t_i^* will become smaller and smaller if we do not increase the width of the neural networks. On the other hand, at the beginning of each iteration, the loss functions will increase. If the time of decrease is very small, the loss function may not decrease to a lower value than in the previous iteration. Identifying an appropriate number of iterations and suitable homotopy parameters will be considered as part of future work.

In summary, HRTA offers two key advantages in training:

- It dynamically builds the activation function, allowing loss functions to resume their decay when the training progress slows down, all without compromising the accuracy of the approximation.

- It accelerates the decay rate by increasing the smallest eigenvalue of Gram matrices with each homotopy iteration. Consequently, it enhances the probability of Gram matrices becoming positive definite in each iteration, further improving the training process.

4 Experimental Results for the Homotopy Relaxation Training Algorithm

In this section, we will use several numerical examples to demonstrate our theoretical analysis results.

4.1 Function approximation by HRTA

In the first part, our objective is to employ NNs to approximate functions of the form $\sin\left(2\pi\sum_{i=1}^d x_i\right)$ for both $d = 1$ and $d = 3$. We will compare the performance of the HRTA method with the Adam optimizer. We used 100 uniform grid points for $d = 1$ and 125 uniform grid points for $d = 3$. Additional experiment details are provided in Appendix. The following Figures 2 and 3 showcase the results achieved using a two-layer neural network with 1000 nodes to approximate $\sin\left(2\pi\sum_{i=1}^d x_i\right)$ for both $d = 1$ and $d = 3$.

Remark 5 We observe oscillations in the figures, which result from plotting the loss against iterations using a logarithmic scale. To mitigate these fluctuations, we decrease the learning rate, allowing the oscillations to gradually diminish during the later stages of training. It's worth noting that these oscillations occur in both the Adam and HRTA optimization algorithms and do not significantly impact the overall efficiency of HRTA.

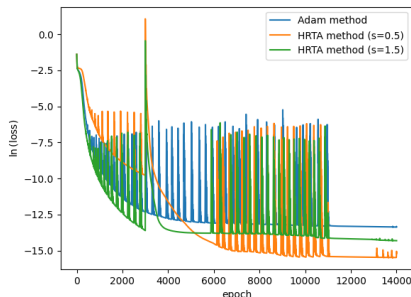


Fig. 2 Approximation for $\sin(2\pi x)$

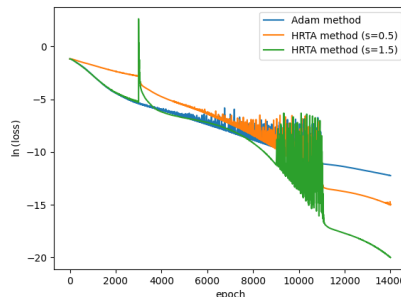


Fig. 3 Approximation for $\sin(2\pi(x_1 + x_2 + x_3))$

In our approach, the HRTA method with $s = 0.5$ signifies that we initially employ $\sigma_{\frac{1}{2}}(x) := \frac{1}{2}\text{Id}(x) + \frac{1}{2}\text{ReLU}(x)$ as the activation functions. We transition to using ReLU as the activation function when the loss function does not decay rapidly. This transition characterizes the homotopy part of our

	Single Layer		Multi Layer	
	Adam	HRTA	Adam	HRTA
200	2.02×10^{-5}	8.72×10^{-7} ($s=1.5$)	2.52×10^{-7}	9.47×10^{-8} ($s=0.5$)
400	6.54×10^{-6}	8.55×10^{-7} ($s=0.5$)	4.83×10^{-8}	1.8×10^{-8} ($s=1.5$)
1000	1.55×10^{-6}	1.88×10^{-7} ($s=0.5$)	2.20×10^{-7}	3.52×10^{-9} ($s=1.5$)

Table 1 Comparisons between HRTA and Adam methods on different NNs.

method. Conversely, the HRTA kernel with $s = 1.5$ signifies that we begin with ReLU as the activation functions and switch to $\sigma_{\frac{3}{2}}(x) := -\frac{1}{2}\text{Id}(x) + \frac{3}{2}\text{ReLU}$ as the activation functions when the loss function does not decay quickly. This transition represents the relaxation part of our method. Based on these experiments, it becomes evident that both cases, $s = 0.5$ and $s = 1.5$, outperform the traditional method in terms of achieving lower error rates. The primary driver behind this improvement is the provision of two opportunities for the loss function to decrease. While the rate of decay in each step may not be faster than that of the traditional method, as observed in the case of $s = 0.5$ for approximating $\sin(2\pi x)$ and $\sin(2\pi(x_1 + x_2 + x_3))$, it's worth noting that the smallest eigenvalue of the training dynamics is smaller than that of the traditional method when $s = 0.5$, as demonstrated in Theorem 1. This is the reason why, in the first step, it decays slower than the traditional method.

In the homotopy case with $s = 0.5$, it can be effectively utilized when we aim to train the ReLU neural network as the final configuration while obtaining a favorable initial value and achieving smaller errors than in the previous stages. Conversely, in the relaxation case with $s = 1.5$, it is valuable when we initially train the ReLU neural network, but the loss function does not decrease as expected. In this situation, changing the activation functions allows the error to start decreasing again without affecting the approximation quality. The advantage of both of these cases lies in their provision of two opportunities and an extended duration for the loss to decrease, which aligns with the results demonstrated in Theorem 2. This approach ensures robust training and improved convergence behavior in various scenarios.

Furthermore, our method demonstrates its versatility as it is not limited to very overparameterized cases or two-layer neural networks. We have shown its effectiveness even in the context of three-layer neural networks and other numbers of nodes (i.e., widths of 200, 400, and 1000). The error rates are summarized in Table 1, and our method consistently outperforms traditional methods.

4.2 Solving partial differential equation by HRTA

In the second part, our goal is to solve the Poisson equation as follows:

$$\begin{cases} -\Delta u(x_1, x_2) = f(x_1, x_2) & \text{in } \Omega, \\ \frac{\partial u}{\partial \nu} = 0 & \text{on } \partial\Omega, \end{cases} \quad (42)$$

using HRTA. Here Ω is a domain within the interval $[0, 1]^2$ and

$$f(x_1, x_2) = \pi^2 [\cos(\pi x_1) + \cos(\pi x_2)].$$

The exact solution to this equation is denoted as $u^*(x_1, x_2) = \cos(\pi x_1) + \cos(\pi x_2)$. We still performed two iterations with 400 sample points and employed 1000 nodes. However, we used the activation function $\bar{\sigma}_{\frac{1}{2}}(x) = \frac{1}{2}\text{Id}(x) + \frac{1}{2}\bar{\sigma}(x)$, where $\bar{\sigma}(x) = \frac{1}{2}\text{ReLU}^2(x)$, which is smoother. Here we consider to solve partial differential equations by Deep Ritz method [47]. In the deep Ritz method, the loss function of the Eq. (42) can be read as

$$\mathcal{E}_D(\boldsymbol{\theta}) := \frac{1}{2} \int_{\Omega} |\nabla \phi(\mathbf{x}; \boldsymbol{\theta})|^2 d\mathbf{x} + \frac{1}{2} \left(\int_{\Omega} \phi(\mathbf{x}; \boldsymbol{\theta}) d\mathbf{x} \right)^2 - \int_{\Omega} f \phi(\mathbf{x}; \boldsymbol{\theta}) d\mathbf{x},$$

where $\boldsymbol{\theta}$ represents all the parameters in the neural network. Here, Ω denotes the domain $[0, 1]^d$. Proposition 1 in [28] establishes the equivalence between the loss function $\mathcal{E}_D(\boldsymbol{\theta})$ and $\|\phi(\mathbf{x}; \boldsymbol{\theta}) - u^*(\mathbf{x})\|_{H^1([0,1]^2)}$, where $u^*(\mathbf{x})$ denotes the exact solution of the PDEs which is $u^*(x_1, x_2) = \cos(\pi x_1) + \cos(\pi x_2)$, and

$$\|f\|_{H^1([0,1]^2)} := \left(\sum_{0 \leq |\alpha| \leq 1} \|D^\alpha f\|_{L^2([0,1]^2)}^p \right)^{1/2}.$$

Therefore, we can use supervised learning via Sobolev training [8, 37, 40] to solve the Poisson equation efficiently and accurately. Our experiments reveal that HRTA remains effective even when $s = 1.5$, as demonstrated in Figures 4 and 5:

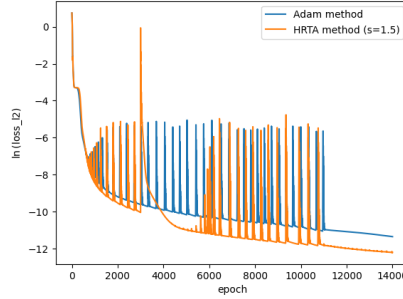
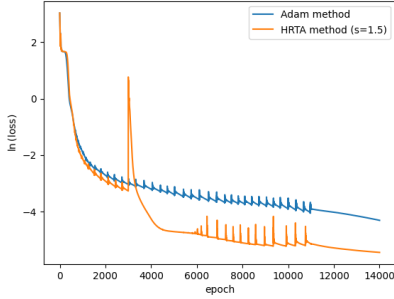


Fig. 4 Loss function in Deep Ritz method **Fig. 5** Solving Eq. (42) measured by L^2 norm

5 Conclusion

In summary, this paper introduces the Homotopy Relaxation Training Algorithm (HRTA), a method designed to expedite gradient descent when it encounters slowdowns. HRTA achieves this by relaxing homotopy activation functions to reshape the energy landscape of loss functions during slow convergence. Specifically, we adapt activation functions to boost the minimum eigenvalue of the gradient descent kernel, thereby accelerating convergence and increasing the likelihood of a positive minimum eigenvalue at each iteration. This paper establishes the theoretical basis for our algorithm, focusing on hyperparameters, while leaving the analysis in a more generalized context for future research.

A Sub-exponential Bernstein's Inequality

Definition 1 ([39]) A random variable X is sub-exponential if and only if its sub-exponential norm is finite i.e.

$$\|X\|_{\psi_1} := \inf\{s > 0 \mid \mathbf{E}_X[e^{|X|/s} \leq 2]\}. \quad (43)$$

Proposition 6 (sub-exponential Bernstein's inequality [39]) Suppose that X_1, \dots, X_m are i.i.d. sub-exponential random variables with $\mathbf{E}X_1 = \mu$, then for any $s \geq 0$ we have

$$\mathbf{P}\left(\left|\frac{1}{m} \sum_{k=1}^m X_k - \mu\right| \geq s\right) \leq 2 \exp\left(-C_0 m \min\left(\frac{s^2}{\|X_1\|_{\psi_1}^2}, \frac{s}{\|X_1\|_{\psi_1}}\right)\right),$$

where C_0 is an absolute constant.

B Function approximation using supervised learning

Example 1 (Approximating $\sin(2\pi x)$) In the first example, our goal is to approximate the function $\sin(2\pi x)$ within the interval $[0, 1]$ using two-layer neural networks (NNs) and the HRTA. We will provide a detailed explanation of the training process for the case of $s = 0.5$, which corresponds to the homotopy training case. The training process is divided into two steps:

1. In the first step, we employ the following approximation function:

$$\phi_{\frac{1}{2}}(x; \boldsymbol{\theta}) := \frac{1}{\sqrt{1000}} \sum_{k=1}^{1000} a_k \sigma_{\frac{1}{2}}(\omega_k x) \quad (44)$$

to approximate the function $\sin(2\pi x)$. Here, $\sigma_{\frac{1}{2}}(x) = \frac{1}{2}\text{Id}(x) + \frac{1}{2}\sigma(x)$, and the initial values of the parameters are drawn from a normal distribution $\boldsymbol{\theta} \sim \mathcal{N}(\mathbf{0}, \mathbf{I})$. We select random sample points (or grid points) $\{x_i\}_{i=1}^{100}$, which are uniformly distributed in the interval $[0, 1]$. The loss function in this step is defined as

$$\mathcal{R}_{S, \frac{1}{2}}(\boldsymbol{\theta}) := \frac{1}{200} \sum_{i=1}^{100} |f(x_i) - \phi_{\frac{1}{2}}(x_i; \boldsymbol{\theta})|^2. \quad (45)$$

Therefore, we employ the Adam optimizer to train this model over 3000 steps to complete the first step of the process.

2. In the second step, we employ the following approximation function:

$$\phi(x; \boldsymbol{\theta}) := \frac{1}{\sqrt{1000}} \sum_{k=1}^{1000} a_k \sigma(\omega_k x) \quad (46)$$

to approximate the function $\sin(2\pi x)$. Here the initial values of the parameters are the results in the first step. The loss function in this step is defined as

$$\mathcal{R}_S(\boldsymbol{\theta}) := \frac{1}{200} \sum_{i=1}^{100} |f(x_i) - \phi(x_i; \boldsymbol{\theta})|^2. \quad (47)$$

Therefore, we employ the Adam optimizer to train this model over 13000 steps to complete the second step of the process and finish the training.

For the purpose of comparison, we employ a traditional method with the following approximation function:

$$\phi(x; \boldsymbol{\theta}) := \frac{1}{\sqrt{1000}} \sum_{k=1}^{1000} a_k \sigma(\omega_k x) \quad (48)$$

to approximate the function $\sin(2\pi x)$. Here, the initial values of the parameters are sampled from a normal distribution $\boldsymbol{\theta} \sim \mathcal{N}(\mathbf{0}, \mathbf{I})$. We select the same random sample points (or grid points) $x_{i=1}^{100}$ as used in the HRTA. The loss function in this step is defined as

$$\mathcal{R}_S(\boldsymbol{\theta}) := \frac{1}{200} \sum_{i=1}^{100} |f(x_i) - \phi(x_i; \boldsymbol{\theta})|^2. \quad (49)$$

Therefore, we employ the Adam optimizer to train this model over 16000 steps to complete the training.

In addition, we conducted experiments with neural networks that were not highly overparameterized, containing only 200 and 400 nodes. The results are illustrated in the following figures:

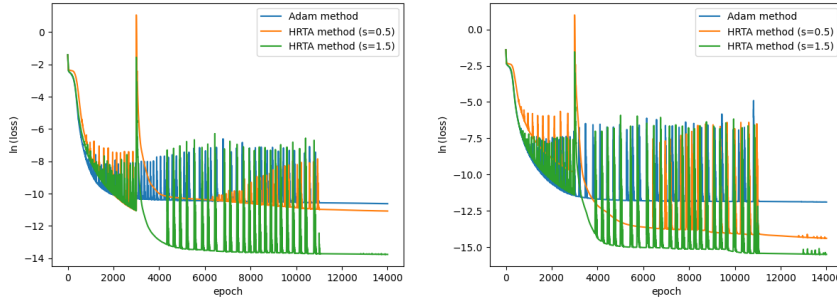


Fig. 6 Approximation for $\sin(2\pi x)$ by NNs with 200 nodes **Fig. 7** Approximation for $\sin(2\pi x)$ by NNs with 400 nodes

Example 2 (Approximating $\sin(2\pi(x_1 + x_2 + x_3))$) The training methods in Example 1 and this current scenario share the same structure. The only difference is that in this case, all instances of ω and x used in Example 1 have been extended to three dimensions. In Figure 3, we demonstrate that HRTA is effective in a highly overparameterized scenario, comprising 125 sample points with 1000 nodes. Additionally, we illustrate that HRTA remains effective in a scenario with less overparameterization, involving 400 nodes and 400 sample points. The results are presented below Figure 8.

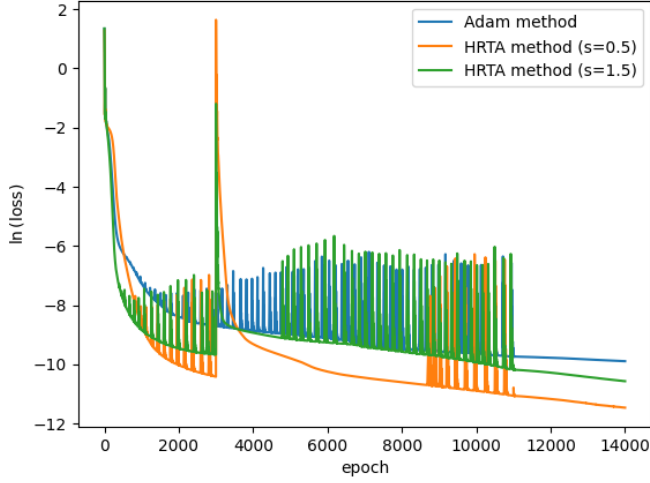


Fig. 8 Approximation for $\sin(2\pi(x_1 + x_2 + x_3))$ with less overparameterization

C Solving partial differential equations

Example 3 In this example, we aim to solve the Poisson equation given by:

$$\begin{cases} -\Delta u(x_1, x_2) = \pi^2 [\cos(\pi x_1) + \cos(\pi x_2)] & \text{in } \Omega, \\ \frac{\partial u}{\partial \nu} = 0 & \text{on } \partial\Omega, \end{cases}$$

by homotopy relaxation training methods and Deep Ritz method [47], where Ω is a domain within the interval $[0, 1]^2$. The exact solution to this equation is denoted as $u^*(x_1, x_2) = \cos(\pi x_1) + \cos(\pi x_2)$.

1. In the first step, we employ the following approximation function:

$$\bar{\phi}(x; \theta) := \frac{1}{\sqrt{1000}} \sum_{k=1}^{1000} a_k \bar{\sigma}(\omega_k x) \quad (50)$$

to solve Poisson equations. Here, $\bar{\sigma}(x) = \frac{1}{2} \text{ReLU}^2(x)$, and the initial values of the parameters are drawn from a normal distribution $\theta \sim \mathcal{N}(\mathbf{0}, \mathbf{I})$. We select random sample points (or grid points) $\{x_i\}_{i=1}^{400}$, which are uniformly distributed in the interval $[0, 1]^2$. As per [28, Proposition 1], the loss function in the Deep Ritz method for solving this Poisson equation is indeed given by:

$$\mathcal{R}_{S, \frac{1}{2}}(\theta) := \frac{1}{800} \sum_{i=1}^{400} [|u^*(x_i) - \bar{\phi}(x_i; \theta)|^2 + |\nabla u^*(x_i) - \nabla \bar{\phi}(x_i; \theta)|^2]. \quad (51)$$

This loss function captures the discrepancy between the exact solution $u^*(x_i)$ and the network's output $\bar{\phi}(x_i; \theta)$, as well as the gradient of the exact solution and the gradient of the network's output, for each sampled point x_i . Therefore, we employ the Adam optimizer to train this model over 16000 steps to complete the step.

2. In the second step, we employ the following approximation function:

$$\bar{\phi}_{\frac{3}{2}}(x; \theta) := \frac{1}{\sqrt{1000}} \sum_{k=1}^{1000} a_k \bar{\sigma}(\omega_k x) \quad (52)$$

to solve Poisson equations. Here the initial values of the parameters are the results in the first step. The loss function in this step is defined as

$$\mathcal{R}_S(\boldsymbol{\theta}) := \frac{1}{800} \sum_{i=1}^{400} \left[|u^*(\mathbf{x}_i) - \bar{\phi}_{\frac{3}{2}}(\mathbf{x}_i; \boldsymbol{\theta})|^2 + |\nabla u^*(\mathbf{x}_i) - \nabla \bar{\phi}_{\frac{3}{2}}(\mathbf{x}_i; \boldsymbol{\theta})|^2 \right]. \quad (53)$$

Therefore, we employ the Adam optimizer to train this model over 13000 steps to complete the step.

References

1. Agostinelli, F., Hoffman, M., Sadowski, P., Baldi, P.: Learning activation functions to improve deep neural networks. arXiv preprint arXiv:1412.6830 (2014)
2. Allen-Zhu, Z., Li, Y., Song, Z.: A convergence theory for deep learning via over-parameterization. In: International conference on machine learning, pp. 242–252. PMLR (2019)
3. Arora, R., Basu, A., Mianjy, P., Mukherjee, A.: Understanding deep neural networks with rectified linear units. arXiv preprint arXiv:1611.01491 (2016)
4. Arora, S., Du, S., Hu, W., Li, Z., Salakhutdinov, R., Wang, R.: On exact computation with an infinitely wide neural net. *Advances in neural information processing systems* **32** (2019)
5. Cao, Y., Gu, Q.: Generalization error bounds of gradient descent for learning over-parameterized deep relu networks. In: Proceedings of the AAAI Conference on Artificial Intelligence, vol. 34, pp. 3349–3356 (2020)
6. Chen, Q., Hao, W.: A homotopy training algorithm for fully connected neural networks. *Proceedings of the Royal Society A* **475**(2231), 20190662 (2019)
7. Chen, Z., Cao, Y., Gu, Q., Zhang, T.: A generalized neural tangent kernel analysis for two-layer neural networks. *Advances in Neural Information Processing Systems* **33**, 13363–13373 (2020)
8. Czarnecki, W., Osindero, S., Jaderberg, M., Swirszcz, G., Pascanu, R.: Sobolev training for neural networks. *Advances in neural information processing systems* **30** (2017)
9. Du, S., Zhai, X., Poczos, B., Singh, A.: Gradient descent provably optimizes over-parameterized neural networks. In: International Conference on Learning Representations (2018)
10. Erhan, D., Courville, A., Bengio, Y., Vincent, P.: Why does unsupervised pre-training help deep learning? In: Proceedings of the thirteenth international conference on artificial intelligence and statistics, pp. 201–208. JMLR Workshop and Conference Proceedings (2010)
11. Gao, T., Liu, H., Liu, J., Rajan, H., Gao, H.: A global convergence theory for deep relu implicit networks via over-parameterization. arXiv preprint arXiv:2110.05645 (2021)
12. Glorot, X., Bordes, A., Bengio, Y.: Deep sparse rectifier neural networks. In: Proceedings of the fourteenth international conference on artificial intelligence and statistics, pp. 315–323. JMLR Workshop and Conference Proceedings (2011)
13. Hao, W.: A homotopy method for parameter estimation of nonlinear differential equations with multiple optima. *Journal of Scientific Computing* **74**, 1314–1324 (2018)
14. Hao, W.: An adaptive homotopy tracking algorithm for solving nonlinear parametric systems with applications in nonlinear odes. *Applied Mathematics Letters* **125**, 107767 (2022)
15. He, J., Tsai, R., Ward, R.: Side effects of learning from low-dimensional data embedded in a euclidean space. *Research in the Mathematical Sciences* **10**(1), 13 (2023)
16. He, K., Zhang, X., Ren, S., Sun, J.: Delving deep into rectifiers: Surpassing human-level performance on imagenet classification. In: Proceedings of the IEEE international conference on computer vision, pp. 1026–1034 (2015)
17. He, K., Zhang, X., Ren, S., Sun, J.: Deep residual learning for image recognition. In: Proceedings of the IEEE conference on computer vision and pattern recognition, pp. 770–778 (2016)

18. Hong, Q., Siegel, J., Tan, Q., Xu, J.: On the activation function dependence of the spectral bias of neural networks. arXiv preprint arXiv:2208.04924 (2022)
19. Huang, W., Liu, C., Chen, Y., Da X., R.Y., Zhang, M., Weng, T.: Analyzing deep pac-bayesian learning with neural tangent kernel: Convergence, analytic generalization bound, and efficient hyperparameter selection. *Transactions on Machine Learning Research* (2023)
20. Jacot, A., Gabriel, F., Hongler, C.: Neural tangent kernel: Convergence and generalization in neural networks. *Advances in neural information processing systems* **31** (2018)
21. Jagtap, A., Kawaguchi, K., Karniadakis, G.: Adaptive activation functions accelerate convergence in deep and physics-informed neural networks. *Journal of Computational Physics* **404**, 109136 (2020)
22. Jagtap, A., Kawaguchi, K., Karniadakis, G.: Locally adaptive activation functions with slope recovery for deep and physics-informed neural networks. *Proceedings of the Royal Society A* **476**(2239), 20200334 (2020)
23. Jagtap, A., Shin, Y., Kawaguchi, K., Karniadakis, G.: Deep kronecker neural networks: A general framework for neural networks with adaptive activation functions. *Neurocomputing* **468**, 165–180 (2022)
24. Keskar, N., Mudigere, D., Nocedal, J., Smelyanskiy, M., Tang, P.: On large-batch training for deep learning: Generalization gap and sharp minima. arXiv preprint arXiv:1609.04836 (2016)
25. Kingma, D., Ba, J.: Adam: A method for stochastic optimization. arXiv preprint arXiv:1412.6980 (2014)
26. Krizhevsky, A., Sutskever, I., Hinton, G.: Imagenet classification with deep convolutional neural networks. *Communications of the ACM* **60**(6), 84–90 (2017)
27. Lu, J., Lu, Y., Nolen, J.: Scaling limit of the stein variational gradient descent: The mean field regime. *SIAM Journal on Mathematical Analysis* **51**(2), 648–671 (2019)
28. Lu, Y., Lu, J., Wang, M.: A priori generalization analysis of the deep ritz method for solving high dimensional elliptic partial differential equations. In: *Conference on learning theory*, pp. 3196–3241. PMLR (2021)
29. Lu, Y., Ma, C., Lu, Y., Lu, J., Ying, L.: A mean field analysis of deep resnet and beyond: Towards provably optimization via overparameterization from depth. In: *International Conference on Machine Learning*, pp. 6426–6436. PMLR (2020)
30. Luo, T., Xu, Z., Ma, Z., Zhang, Y.: Phase diagram for two-layer relu neural networks at infinite-width limit. *The Journal of Machine Learning Research* **22**(1), 3327–3373 (2021)
31. Mastromichalakis, S.: Alrelu: A different approach on leaky relu activation function to improve neural networks performance. arXiv preprint arXiv:2012.07564 (2020)
32. Morgan, A., Sommese, A.: Computing all solutions to polynomial systems using homotopy continuation. *Applied Mathematics and Computation* **24**(2), 115–138 (1987)
33. Seleznova, M., Kutyniok, G.: Neural tangent kernel beyond the infinite-width limit: Effects of depth and initialization. In: *International Conference on Machine Learning*, pp. 19522–19560. PMLR (2022)
34. Siegel, J.: Accelerated optimization with orthogonality constraints. *Journal of Computational Mathematics* **39**(2), 207 (2021)
35. Siegel, J., Hong, Q., Jin, X., Hao, W., Xu, J.: Greedy training algorithms for neural networks and applications to pdes. arXiv preprint arXiv:2107.04466 (2021)
36. Sommese, A., Wampler, C.: *The Numerical solution of systems of polynomials arising in engineering and science*. World Scientific (2005)
37. Son, H., Jang, J., Han, W., Hwang, H.: Sobolev training for the neural network solutions of PDEs. arXiv preprint arXiv:2101.08932 (2021)
38. Sun, T., Li, D., Wang, B.: Adaptive random walk gradient descent for decentralized optimization. In: *International Conference on Machine Learning*, pp. 20790–20809. PMLR (2022)
39. Vershynin, R.: *High-dimensional probability: An introduction with applications in data science*, vol. 47. Cambridge university press (2018)
40. Vlassis, N., Sun, W.: Sobolev training of thermodynamic-informed neural networks for interpretable elasto-plasticity models with level set hardening. *Computer Methods in Applied Mechanics and Engineering* **377**, 113695 (2021)

41. Wang, B., Ye, Q.: Stochastic gradient descent with nonlinear conjugate gradient-style adaptive momentum. arXiv preprint arXiv:2012.02188 (2020)
42. Whiting, W., Wang, B., Xin, J.: Convergence of hyperbolic neural networks under riemannian stochastic gradient descent. *Communications on Applied Mathematics and Computation* pp. 1–14 (2023)
43. Wu, S., Zhong, S., Liu, Y.: Deep residual learning for image steganalysis. *Multimedia tools and applications* **77**, 10437–10453 (2018)
44. Xu, J., Li, Z., Du, B., Zhang, M., Liu, J.: Reluplex made more practical: Leaky relu. In: 2020 IEEE Symposium on Computers and communications (ISCC), pp. 1–7. IEEE (2020)
45. Yang, G., Littwin, E.: Tensor programs iib: Architectural universality of neural tangent kernel training dynamics. In: International Conference on Machine Learning, pp. 11762–11772. PMLR (2021)
46. You, Y., Li, J., Reddi, S., Hseu, J., Kumar, S., Bhojanapalli, S., Song, X., Demmel, J., Keutzer, K., Hsieh, C.: Large batch optimization for deep learning: Training bert in 76 minutes. arXiv preprint arXiv:1904.00962 (2019)
47. Yu, B., E, W.: The deep ritz method: a deep learning-based numerical algorithm for solving variational problems. *Communications in Mathematics and Statistics* **6**(1), 1–12 (2018)
48. Zhang, Y., Xu, Z.J., Luo, T., Ma, Z.: A type of generalization error induced by initialization in deep neural networks. In: Mathematical and Scientific Machine Learning, pp. 144–164. PMLR (2020)